Ex-vivo explant culture of NSCLC provides a relevant preclinical model for evaluation of primary tumour responses to anti-cancer therapies

Ellie Karekla[1], Wen-Jing Liao[1], Barry Sharp[2], John Pugh[2], Helen Reid[2], John Le Quesne[1,3], David Moore[1], Catrin Pritchard[1], Marion MacFarlane[3], J Howard Pringle[1]

[1]Department of Cancer Studies, University of Leicester, Leicester LE2 7LX, UK

[2]Centre for Analytical Science, Department of Chemistry, Loughborough University, Loughborough, Leicestershire LE11 3TU, UK

[3]MRC Toxicology Unit, Hodgkin Building, Lancaster Road, Leicester LE1 9HN, UK

Note: Supplementary data for this article are available at Cancer Research Online

C.Pritchard, M.MacFarlane, and J.H.Pringle contributed equally to this article.

Running title: Evaluation of tumour drug responses using a novel ex-vivo platform

Key words: NSCLC, explants, chemotherapy, TRAIL, TP53

Word count 5,867, Figures and tables: 6 figures and 1 table, 43 references

***Corresponding authors**: Catrin Pritchard, Department of Cancer Studies, University of Leicester, Lancaster Road, Leicester LE1 9HN, UK (e-mail: cap8@le.ac.uk), Marion MacFarlane, MRC Toxicology Unit, Hodgkin Building, Lancaster Road, Leicester LE1 9HN, UK (e-mail: mm21@le.ac.uk), Howard Pringle, Department of Cancer Studies, University of Leicester, Lancaster Road, Leicester LE1 9HN, UK (e-mail: jhp@le.ac.uk)

The authors declare no potential conflicts of interest

Abstract

Non-Small Cell Lung Cancer (NSCLC) is a highly resistant cancer with only ~30% of tumours responding to first-line cisplatin chemotherapy following surgery. To improve treatment outcomes, preclinical models are urgently required that better predict individual patient response to novel therapies. Using freshly resected tumour tissue, we have established an optimal *ex-vivo* NSCLC explant culture model that enables concurrent evaluation of tumour cell response to therapy while maintaining the tumour microenvironment. We show that ~70% of NSCLC samples are amenable to explant culture and tissue integrity is retained intact for up to 72 hours. As proof of principle we examined explant response to cisplatin and identified differential sensitivity with ~50% of cases responding to the drug *ex-vivo*. Importantly, there was a significant relationship between cisplatin response in explants and patient survival (P=0.019). By evaluating Platinum (Pt) ion distribution directly on explant tissue, we found that resistant tumours exclude Pt ions from tumour areas in contrast to sensitive tumours. Intact TP53 did not predict cisplatin response but, instead, showed a positive correlation between cisplatin sensitivity and *TP53* mutation (P<0.0003). Treatment of NSCLC explants with the targeted agent TRAIL revealed differential sensitivity with the majority of tumours resistant to single or cisplatin combined therapy. Thus, we have validated a rapid, reproducible and low-cost platform for assessing drug responses in patient tumours *ex-vivo* and show that our results have clinical relevance. This technology has significant potential for preclinical testing of novel drugs and for stratifying patients using biomarker evaluation.

Introduction

NSCLC is a leading cause of cancer death worldwide. Patients with Stage I-III tumours are treated with surgery and adjuvant chemotherapy or radiotherapy whereas patients with Stage IV disease receive palliative chemotherapy alone. Most patients receive combination chemotherapy based on clinical parameters of cisplatin or carboplatin with at least one other drug such as Vinorelbine, Gemcitabine or Paclitaxel. Unfortunately, only ~30% of tumours respond to first-line chemotherapy following surgery (1) and thus outcomes for the majority of patients are dismal.

The era of personalized medicine has heralded the development of targeted therapies for NSCLC, some of which rely on pre-selection of cancers according to genetic mutation. For example, selective EGFR inhibitors gefitinib and erlotinib provide clinical benefit over standard chemotherapy for NSCLC tumours bearing *EGFR* mutations (2,3) while the ALK inhibitor crizotinib benefits *ALK*-mutated cases (4). A global industry is centred on assessing additional mono- or combinatorial treatments in NSCLC clinical trials. Despite this momentum, late-stage failures are a reality and there is <11% success in bringing a drug to market (5), attributable in part to non-predictive preclinical drug platforms (6,7). The incorporation of Patient-Derived Xenograft (PDX) mouse models (8,9) into preclinical studies has improved predictive accuracy somewhat (10,11). However, PDX efficacy studies are expensive, requiring large numbers of mice. Furthermore, not all primary human tumours generate PDXs and, of those that do, serial propagation can select tumours that adapt to grow in an immunocompromised environment.

An alternative approach is to use three-dimensional *ex-vivo* culture of fresh human tumours. Methods for *ex-vivo* culture of human tumours have been available for many years and evidence shows that they can reliably reflect tumour growth *in vivo* (12-17). Here, we have developed and perfected an *ex-vivo* culture method for NSCLC tumour samples that is both simple and reproducible. We have optimized culture conditions and show that tumour and stroma are retained and viable. As proof of concept, NSCLC explant response to the standard-of-care chemotherapy drug cisplatin was examined as well as response to the targeted agent TRAIL. We also illustrate how explants can be used to inform mechanisms of drug action by evaluating biomarkers of drug response. Together our data show the explant platform can effectively predict patient response to therapy and can be used for monitoring clinically-relevant biomarkers.

Materials and Methods

Ex-vivo explant culture

Fresh NSCLC tumours were collected from consented patients undergoing lung surgery (Ethical approval: LREC: 07/MRE08/07). Patients had no prior exposure to chemotherapy. Viable tumour areas were identified by frozen tissue sectioning and Haematoxylin and Eosin (H&E) staining. Tissue was placed in Hank's Balanced Salt Solution and cut into fragments of 2-3 mm^3 using two skin graft blades on a dental wax surface. These were placed in fresh culture media (DMEM with 4.5 g/L Glucose plus 0-5% FCS and 1% pen/strep); nine fragments were randomly selected and placed on a 0.4 μm culture insert disc (Millipore) floated on 1.5 ml of media in a 6-well dish. Explants were incubated at 37°C and 5% CO_2 for 16-20 hours. Discs were then transferred to new wells containing 1.5 ml fresh media and drugs or carrier control were added to each well in a volume of 1.5 μl for 24 hours. Cisplatin (Sigma) was utilized over a dose range of 0-50 μM (dissolved in dimethylformamide). TRAIL (18,19) was utilized at 1 μg/ml, diluted in DMEM media from a stock of 1 mg/ml. After treatment, explants were washed with PBS and transferred to new wells containing 1 ml of 4% (w/v) paraformaldehyde for 20 hours. Explants were transferred onto sponges, pre-soaked in 70% (v/v) ethanol and placed in histology cassettes. They were embedded into paraffin blocks from which 4 μm sections were generated.

Histological analysis

H&E staining of formalin-fixed, paraffin-embedded (FFPE) material sections were generated by standard approaches and, for immunohistochemistry, sections were processed as described (20). The Novolink™ Polymer Detection system kit (Leica Microsystems, UK) was used according to the manufacturer's instructions. Primary antibodies were: Cleaved PARP [E51]: Abcam 1:6000, Ki-67 Clone MIB-1: DAKO 1:2000, p53 DO1: gift from David Lane 1:1000, Cytokeratin clone MNF116: DAKO 1:5000. Antibodies were diluted in blocking solution made with 3% (w/v) Bovine Serum Albumin, 0.1% (v/v) Triton X-100 (Fisons, UK) in TBS. Staining was visualised under a LEICA DM 2500 microscope and photographed with a LEICA DFC 420 camera.

Quantitation of immunohistochemical staining

Images of the tumour explants were taken at 10x magnification and merged using Adobe Photoshop CS5.1, generating a single image of one explant. Tumour area was determined using Image J analysis (21), excluding areas of necrosis and stroma. The labelling index was determined

using ImmunoRatio (22) and a single value was obtained for all nine explants derived from one treatment that was expressed as a percentage of the total tumour area.

Laser Ablation Inductively Coupled Plasma Mass Spectrometry (LA-ICP-MS)

Sections of explants treated with cisplatin were subjected LA-ICP-MS to produce elemental maps showing the spatial distribution of Platinum (Pt) in tissue sections (23). The method is described in Supplementary Fig. S1.

Statistical analysis

Significance of proliferation/death indices was determined by Wilcoxon matched pairs test and Jonckheere-Terpstra trend test, respectively. Unpaired data were compared by the Mann-Whitney U test or Kruskal-Wallis one-way ANOVA. Paired data were analyzed by the Page L test (Unistat Statistical Package, version 5.0, Unistat) and interrelationships were investigated by Spearman rank correlation (SPSS, version 22, IBM). The optimal cut-off point to determine the relationship between explant response and patient survival was examined using a plot of sensitivity against 1-specificity as a Receiver Operator Characteristic (ROC) curve (SPSS). Survival was investigated by Kaplan-Meier analysis (SPSS) of cell indices, which were compared by the log rank Mantel-Haenzel (Peto) test, and by univariate and multivariate Cox regression (SPSS). P values of <0.05 were considered statistically significant.

Results

Histopathology of NSCLC tumours used for explants

Table 1 provides a summary of patient demographics, tumour type and stage for all 41 samples utilized for this study. The histological types and stages were broadly consistent with the known distribution of NSCLC cases in the UK (24). A proportion of NSCLC tumours are known to be necrotic (25) and an important first step was to exclude such tumours from analysis using H&E assessment. This led to the identification of 13 tumours (~32%) that were excluded from explant generation. Supplementary Fig. S2 indicates the histological type (Supplementary Fig. S2A) and stage (Supplementary Fig. S2B) of viable and non-viable tumours. The highest proportion of non-viable tumours was within the adenocarcinoma (ADC) subtype (~44% compared to ~25% of Squamous Cell Carcinoma (SCC) cases). However, there was no correlation between tumour stage and viability.

28 viable tumours were processed for explant culture. Intrinsic levels of cell proliferation and cell death were first assessed in uncultured samples by Ki67 or cleaved PARP (cPARP) immunostaining (Fig. 1A, B). SCC tumours displayed significantly higher levels of proliferation than ADC, while Atypical Carcinoid (AC) tumours were essentially indolent (Fig. 1A). These observations are consistent with several previous reports (26-28). With regard to cPARP staining, the majority of samples showed <20% of staining, indicating low levels of intrinsic cell death (Fig. 1A, B).

Optimisation of explant culture

Our approach for the NSCLC explant culture system was based on previous experience with breast cancer samples (29, Naik *et al.* under review). As a first step in implementing protocols for NSCLC, we first investigated the effects of culture time and FCS concentration.

Explants were routinely allowed to recover for a period of 16-20 hours after their initial generation; viability was assessed over a time range of 24-72 hours after recovery for five tumours. As shown in Fig. 2A, a trend of decreasing cell proliferation and increasing cell death with increasing time of culture was observed suggesting *ex-vivo* explant cultures are more viable in short term culture. Varying FCS concentration, from 0-5%, at 24 hours of culture after the initial 16-20 hours of culture recovery showed no statistically significant difference in levels of proliferation or cell death (Fig. 2B).

The data from above suggest that the 24-hour time point gives the greatest viability, but that FCS concentration is not a significant factor. Subsequent analyses of drug responses were therefore performed for 24 hours, using 1% as the standard FCS concentration. Pooled data for 21 explants under these conditions are shown in Fig. 2C. Overall, there is a small but significant effect of cultivation on explant viability, with there being a ~10% decrease in proliferation and a ~10% increase in cell death compared to the uncultured but freshly fixed native tumour.

Explant responses to cisplatin

17 explants were treated with a dose range of cisplatin (0-50 μM) for 24 hours following the initial recovery of 16-20 hours. Data for individual cases are shown in Supplementary Fig. S3. Levels of cell proliferation were only marginally affected by the drug (Supplementary Fig. S3B) and therefore the emphasis was placed on assessing cell death responses (Supplementary Fig. S3A). Cell death response for each tumour was calculated as fold-induction relevant to the control over the dose range (Fig. 3A). 8/17 (47%) tumours showed no response to the drug whereas the remaining 9/17 (53%) showed cell death induction ranging from 2-25 fold. The majority of these tumours only showed a response at high levels of cisplatin (50 μM), with only two tumours (LT88 and LT92) responding at the lower dose of 10 μM.

In addition to the 17 explants treated with a dose range of cisplatin, a further 9 were treated with a single dose of 50 μM cisplatin. We obtained clinical and histopathology information on all 26 patients and their tumours (Supplementary Table S1). Cell death difference compared to control in response to cisplatin is included alongside this information. One tumour was excluded from analysis due to complex histopathology. For the remaining 25, a ROC curve was used to determine the threshold for resistance/sensitivity to cisplatin and this analysis gave an area under the curve of 0.764 ± 0.098 SE (P=0.031), a likelihood ratio of 3.56 and identified 28.5% as the optimal cutoff (Supplementary Fig. S4A).

We then categorized each explant into being either sensitive or resistant to cisplatin (Supplementary Fig. S4B and Table S1). Using clinical information on corresponding patients (Table S1), the relationship of cisplatin sensitivity/resistance in explant culture to patient survival post-surgery was determined (Fig. 3B). The data show a statistically significant relationship (P=0.019) with sensitive cases demonstrating a Mean Survival Time (MST) of 44 months and resistant cases a MST of 26 months. Cisplatin sensitivity in explants was also correlated with tumour stage and

histological type (Fig. 3C). There was a significant negative trend between difference in %cPARP staining compared to control in response to cisplatin and increasing tumour stage suggesting more advanced tumours are more resistant to the drug. There was also a significant correlation between cisplatin sensitivity and tumour type with SCC cases demonstrating greater cisplatin sensitivity than either ADC or AC subtypes, with AC subtypes being particularly resistant to the drug (Fig. 3C).

Cisplatin sensitivity is linked to drug accumulation in tumour areas

A number of mechanisms have been reported to render cells resistant to cisplatin including reduced drug uptake, enhanced export, drug deactivation, increased repair of DNA damage or alterations in apoptosis (30,31). To examine drug uptake/export, we investigated Pt ion distribution across explant tissue using LA-ICP-MS (see Fig. S1) imaging (Fig. 5 and Supplementary Fig. S5). For sensitive cases, Pt ions were present throughout the tumour and stromal areas of the explant indicating widespread cisplatin uptake (Figure 4B and S5). In contrast, for resistant cases, Pt ions were depleted from areas corresponding to tumour cells but were present in the stroma (Fig. 4A and Supplementary Fig. S5). Thus, whilst cisplatin is available to the resistant explants, there is decreased intracellular drug concentration in tumour cells.

TP53 expression in the explants

The *TP53* gene is frequently mutated in NSCLC (31). Wild-type TP53 protein is induced by DNA damaging agents such as cisplatin, whereas mutated TP53 is either not expressed or is constitutively expressed. We utilized immunohistochemistry to gain an indication of TP53 function in the 26 tumours, identifying three categories: a) ^{WT}TP53 tumours (10 tumours), b) ^{MUT}TP53 tumours with constitutively high TP53 levels (14 tumours), c) ^{MUT}TP53 tumours expressing undetectable TP53 (2 tumours). Immunohistochemical TP53 staining of positive and negative tumours is shown in Fig. 5A while Fig. 5B indicates induction of TP53 following treatment of a ^{WT}TP53 tumour with a dose range of cisplatin and quantitation of the staining. Overall, 38.5% of tumours were ^{WT}TP53 and 61.5% ^{MUT}TP53 based on immunohistochemical criteria (Supplementary Table S1). This is approximately consistent with the known mutation rate of *TP53* in human NSCLC (32).

As expected, TP53^{MUT} tumours had significantly higher intrinsic levels of proliferation compared with TP53^{WT} tumours (Fig. 5C), and the majority of TP53^{MUT} cancers were of the SCC subtype (Fig.

5D). In terms of response to cisplatin, $TP53^{MUT}$ samples had significantly higher levels of cell death induction compared to $TP53^{WT}$ samples (Fig. 5D, left), and significantly higher levels of suppression of cell proliferation (Fig. 5D, right). These data counteract the view that $TP53^{MUT}$ tumours are defective in their apoptotic response to DNA damage induced by cisplatin.

Explant responses to TRAIL

TRAIL is a death receptor ligand that has been developed for therapy although clinical trials have been disappointing (33). It is thought that preclinical *in vitro* studies using cell lines have not faithfully represented the clinical situation. This is supported by data demonstrating that the majority of primary human tumour cells are resistant to TRAIL receptor agonist (33-35). To investigate TRAIL sensitivity in NSCLC, 12 explants were treated with TRAIL either as a single agent or in combination with cisplatin (Fig. 6A). TRAIL alone did not elicit a strong response, except for one case (LT22) that demonstrated ~4-fold induction of cell death. Similarly, TRAIL did not enhance the effects of cisplatin in the majority of cases, except for one tumour (LT83) for which slightly greater cell death induction (6-fold) than cisplatin alone (4-fold) was detected (Fig. 6A, B).

Discussion

Predicting drug response in cancer patients is a major challenge in the clinic. Cell line-xenograft mouse models have been extensively used for preclinical drug testing but, while these models can provide an initial indication of *in vivo* drug efficacy, data is often not predictive of patient outcome (6,36). Although the advent of mouse PDX models has opened up the possibility of tailoring drugs to a tumour with a specific genetic lesion (10,37), in practice these models are expensive and lose the characteristics of the original human tumour microenvironment over time. Here, we have perfected a rapid and low cost platform that relies on the *in situ* assessment of drug responses within real human tumours. We validate this platform by showing that explant response to the standard-of-care chemotherapy drug cisplatin is related to survival of patients who also receive this drug after surgery (P=0.019). Responses to the targeted agent TRAIL are also more consistent with clinical outcomes than standard cell line model systems (29, 33-35). We demonstrate how the explant platform can be used to inform mechanisms of drug action by biomarker monitoring.

A number of organotypic culture systems have been previously developed for human tumours (12-17). In most of these previous systems, viability of tumours has been demonstrated for up to 7 days (12-17). Here, we identified a mild effect of cultivation after 24 hours of culture (Fig. 2C), but tissue architecture was maintained intact for up to 72 hours. Our preference is to examine drug responses immediately after cultivation in order to minimize any effects of culture. Correlation of organotypic culture data with patient outcomes has been previously reported for the Histoculture Drug Response Assay system (14-16). However, a disadvantage of this technique is that the end-point requires enzymatic digestion of tissue, thus preventing assessment of the specific cell type affected by the drug. This disadvantage can be overcome by using our *in situ* FFPE/immunohistochemical approach.

Our data show that the majority of the cisplatin-resistant tumours are of a higher stage (Fig. 3) but the ability to induce cell death in response to cisplatin does not correlate with intact TP53 (Fig. 5). In fact, we have found that *TP53*-mutated NSCLC cases are more sensitive to cisplatin in explants than ^{WT}TP53 cases (Fig. 5D). Previous studies have investigated whether *TP53* mutations are of prognostic value in predicting response to chemotherapy in NSCLC; the results are controversial (38). In a 35 patient study, the presence of mutant TP53 was highly indicative of resistance to cisplatin (P<0.002) (39) while in a study of 253 patients, TP53-positive patients had a significantly greater survival benefit from adjuvant chemotherapy compared with TP53-negative patients (40).

Another report in the International Adjuvant Lung Cancer Trial (IALT), a randomized trial of adjuvant cisplatin-based chemotherapy, found no correlation between *TP53* mutation and outcome in 524 patients (41). Overall it will be important to extend analysis to a greater number of explants/patients in order to robustly determine the prognostic value of *TP53* mutation. Lack of response to cisplatin does, however, correlate with exclusion of the drug from tumour areas (Fig. 4). Cisplatin import is mediated by the copper transporter CTR1, while the copper transporters ATP7A and ATP7B regulate the efflux of cisplatin (42). Resistance to cisplatin has been associated with alterations in the expression status of these transporters (43) and so it will also be important to evaluate these transporters in the explant system used here.

In summary, the explant platform provides a patient-relevant model system for the preclinical evaluation of novel anticancer agents. When combined with tumour stratification approaches, the platform has the potential for personalizing drug treatment. The technology is low-cost, rapid and achievable within an integrated cancer translational research setting.

Authors' Contributions

Conception and design: C.Pritchard, M.MacFarlane, J.H.Pringle.

Development of methodology: E.Karekla, C.Pritchard, M.MacFarlane, J.H.Pringle, B.Sharp

Acquisition of data: E.Karekla, W-J.Liao, J.Pugh, H.Reid, J.Le Quesne, D.Moore

Writing, review and/or revision of manuscript: E.Karekla, C.Pritchard, M.MacFarlane, J.H.Pringle, B.Sharp, J.Le Quesne, D.Moore.

Acknowledgements

We thank Andrew Wardlaw for providing the ethical framework for this project, Hilary Marshall and Will Monteiro for support in tissue collection, and thoracic surgeons at Glenfield Hospital, Leicester. We also thank Angie Gillies for assistance with histology. CP was supported by a Royal Society-Wolfson Merit Award.

Financial support

This work was supported by a Medical Research Council (MRC) Doctoral Training Grant to EK, the MRC Toxicology Unit (MC A/600), and the Leicester Experimental Cancer Medicine Centre (C325/A15575 Cancer Research UK/UK Department of Health).

References

1. Ardizzoni A, Boni L, Tiseo M, Fossella FV, Schiller JH, Paesmans M, et al. Cisplatin- versus carboplatin-based chemotherapy in first-line treatment of advanced non-small-cell lung cancer: an individual patient data meta-analysis. J Natl Cancer Inst 2007;99(11):847-57.

2. Mok TS, Wu YL, Thongprasert S, Yang CH, Chu DT, Saijo N, et al. Gefitinib or carboplatin-paclitaxel in pulmonary adenocarcinoma. N Engl J Med 2009;361(10):947-57.

3. Rosell R, Molina MA, Serrano MJ. EGFR mutations in circulating tumour DNA. Lancet Oncol 2012;13(10):971-3.

4. Solomon BJ, Mok T, Kim DW, Wu YL, Nakagawa K, Mekhail T, et al. First-line crizotinib versus chemotherapy in ALK-positive lung cancer. N Engl J Med 2014;371(23):2167-77.

5. Kola I, Landis J. Can the pharmaceutical industry reduce attrition rates? Nat Rev Drug Discov 2004;3(8):711-5.

6. Johnson JI, Decker S, Zaharevitz D, Rubinstein LV, Venditti JM, Schepartz S, et al. Relationships between drug activity in NCI preclinical in vitro and in vivo models and early clinical trials. Br J Cancer 2001;84(10):1424-31.

7. Fricker J. Time for reform in the drug-development process. Lancet Oncol 2008;9(12):1125-6.

8. Tentler JJ, Tan AC, Weekes CD, Jimeno A, Leong S, Pitts TM, et al. Patient-derived tumour xenografts as models for oncology drug development. Nat Rev Clin Oncol 2012;9(6):338-50.

9. Siolas D, Hannon GJ. Patient-derived tumor xenografts: transforming clinical samples into mouse models. Cancer Res 2013;73(17):5315-9.

10. Hidalgo M, Bruckheimer E, Rajeshkumar NV, Garrido-Laguna I, De Oliveira E, Rubio-Viqueira B, et al. A pilot clinical study of treatment guided by personalized tumorgrafts in patients with advanced cancer. Mol Cancer Ther 2011;10(8):1311-6.

11. Bertotti A, Migliardi G, Galimi F, Sassi F, Torti D, Isella C, et al. A molecularly annotated platform of patient-derived xenografts ("xenopatients") identifies HER2 as an effective therapeutic target in cetuximab-resistant colorectal cancer. Cancer Discov 2011;1(6):508-23.

12. Pampaloni F, Reynaud EG, Stelzer EH. The third dimension bridges the gap between cell culture and live tissue. Nat Rev Mol Cell Biol 2007;8(10):839-45.

13. Freeman AE, Hoffman RM. In vivo-like growth of human tumors in vitro. Proc Natl Acad Sci U S A 1986;83(8):2694-8.

14. Yoshimasu T, Oura S, Hirai I, Tamaki T, Kokawa Y, Hata K, et al. Data acquisition for the histoculture drug response assay in lung cancer. J Thorac Cardiovasc Surg 2007;133(2):303-8.

15. Kubota T, Sasano N, Abe O, Nakao I, Kawamura E, Saito T, et al. Potential of the histoculture drug-response assay to contribute to cancer patient survival. Clin Cancer Res 1995;1(12):1537-43.

16. Furukawa T, Kubota T, Hoffman RM. Clinical applications of the histoculture drug response assay. Clin Cancer Res 1995;1(3):305-11.

17. Vaira V, Fedele G, Pyne S, Fasoli E, Zadra G, Bailey D, et al. Preclinical model of organotypic culture for pharmacodynamic profiling of human tumors. Proc Natl Acad Sci U S A 2010;107(18):8352-6.

18. Harper N, MacFarlane M. Recombinant TRAIL and TRAIL receptor analysis. Methods Enzymol 2008;446:293-313.

19. MacFarlane M, Ahmad M, Srinivasula SM, Fernandes-Alnemri T, Cohen GM, Alnemri ES. Identification and molecular cloning of two novel receptors for the cytotoxic ligand TRAIL. J Biol Chem 1997;272(41):25417-20.

20. Caramel J, Papadogeorgakis E, Hill L, Browne GJ, Richard G, Wierinckx A, et al. A switch in the expression of embryonic EMT-inducers drives the development of malignant melanoma. Cancer Cell 2013;24(4):466-80.

21. Schneider CA, Rasband WS, Eliceiri KW. NIH Image to ImageJ: 25 years of image analysis. Nat Methods 2012;9(7):671-5.

22. Tuominen VJ, Ruotoistenmaki S, Viitanen A, Jumppanen M, Isola J. ImmunoRatio: a publicly available web application for quantitative image analysis of estrogen receptor (ER), progesterone receptor (PR), and Ki-67. Breast Cancer Res 2010;12(4):R56.

23. Koppen C, Reifschneider O, Castanheira I, Sperling M, Karst U, Ciarimboli G. Quantitative imaging of platinum based on laser ablation-inductively coupled plasma-mass spectrometry to investigate toxic side effects of cisplatin. Metallomics 2015;7(12):1595-603.

24. Baldwin DR, White B, Schmidt-Hansen M, Champion AR, Melder AM, Guideline Development G. Diagnosis and treatment of lung cancer: summary of updated NICE guidance. BMJ 2011;342:d2110.

25. Swinson DE, Jones JL, Richardson D, Cox G, Edwards JG, O'Byrne KJ. Tumour necrosis is an independent prognostic marker in non-small cell lung cancer: correlation with biological variables. Lung Cancer 2002;37(3):235-40.

26. Mehdi SA, Etzell JE, Newman NB, Weidner N, Kohman LJ, Graziano SL. Prognostic significance of Ki-67 immunostaining and symptoms in resected stage I and II non-small cell lung cancer. Lung Cancer 1998;20(2):99-108.

27. Nguyen VN, Mirejovsky P, Mirejovsky T, Melinova L, Mandys V. Expression of cyclin D1, Ki-67 and PCNA in non-small cell lung cancer: prognostic significance and comparison with p53 and bcl-2. Acta Histochem 2000;102(3):323-38.

28. Warth A, Cortis J, Soltermann A, Meister M, Budczies J, Stenzinger A, et al. Tumour cell proliferation (Ki-67) in non-small cell lung cancer: a critical reappraisal of its prognostic role. Br J Cancer 2014;111(6):1222-9.

29. Twiddy D, Edwards J, Walker RA, Cohen GM, MacFarlane M. A TRAIL-R1-specific ligand in combination with doxorubicin selectively targets primary breast tumour cells for apoptosis. Breast Cancer Research 2010;12(Suppl.1):17-18.

30. Kelland LR. Preclinical perspectives on platinum resistance. Drugs 2000;59 Suppl 4:1-8; discussion 37-8.

31. Cosaert J, Quoix E. Platinum drugs in the treatment of non-small-cell lung cancer. Br J Cancer 2002;87(8):825-33.

32. Le Calvez F, Mukeria A, Hunt JD, Kelm O, Hung RJ, Taniere P, et al. TP53 and KRAS mutation load and types in lung cancers in relation to tobacco smoke: distinct patterns in never, former, and current smokers. Cancer Res 2005;65(12):5076-83.

33. Amarante-Mendes GP, Griffith TS. Therapeutic applications of TRAIL receptor agonists in cancer and beyond. Pharmacol Ther 2015;155:117-31.

34. Dyer MJ, MacFarlane M, Cohen GM. Barriers to effective TRAIL-targeted therapy of malignancy. J Clin Oncol 2007;25(28):4505-6.

35. MacFarlane M, Kohlhaas SL, Sutcliffe MJ, Dyer MJ, Cohen GM. TRAIL receptor-selective mutants signal to apoptosis via TRAIL-R1 in primary lymphoid malignancies. Cancer Res 2005;65(24):11265-70.

36. Kung AL. Practices and pitfalls of mouse cancer models in drug discovery. Adv Cancer Res 2007;96:191-212.

37. Aparicio S, Hidalgo M, Kung AL. Examining the utility of patient-derived xenograft mouse models. Nat Rev Cancer 2015;15(5):311-6.

38. Toyooka S, Tsuda T, Gazdar AF. The TP53 gene, tobacco exposure, and lung cancer. Hum Mutat 2003;21(3):229-39.

39. Kandioler D, Stamatis G, Eberhardt W, Kappel S, Zochbauer-Muller S, Kuhrer I, et al. Growing clinical evidence for the interaction of the p53 genotype and response to induction chemotherapy in advanced non-small cell lung cancer. J Thorac Cardiovasc Surg 2008;135(5):1036-41.

40. Tsao MS, Aviel-Ronen S, Ding K, Lau D, Liu N, Sakurada A, et al. Prognostic and predictive importance of p53 and RAS for adjuvant chemotherapy in non small-cell lung cancer. J Clin Oncol 2007;25(33):5240-7.

41. Ma X, Rousseau V, Sun H, Lantuejoul S, Filipits M, Pirker R, et al. Significance of TP53 mutations as predictive markers of adjuvant cisplatin-based chemotherapy in completely resected non-small-cell lung cancer. Mol Oncol 2014;8(3):555-64.

42. Safaei R, Howell SB. Copper transporters regulate the cellular pharmacology and sensitivity to Pt drugs. Crit Rev Oncol Hematol 2005;53(1):13-23.

43. Kuo MT, Chen HH, Song IS, Savaraj N, Ishikawa T. The roles of copper transporters in cisplatin resistance. Cancer Metastasis Rev 2007;26(1):71-83.

Figure Legends

Figure 1. Intrinsic levels of proliferation and apoptosis in the tumours used for explants. A, Proliferation was assessed by quantitating Ki67 immunohistochemical staining and cell death by quantitating cPARP staining. The left panel indicates the % of intrinsic proliferation and cell death in tumours. A single dot represents a single tumour sample. For the Ki67 staining, the samples were grouped into one of three groups: H = High (>40%), M = Medium (20-40%), L = Low (0-20%). The samples all had low intrinsic levels of cPARP staining. The middle and right panels indicate the % Ki67 and % cPARP staining for tumours with ADC, SCC and AC histologies. The SCC samples had significantly higher levels of intrinsic proliferation compared to the ADC samples whereas the AC samples were indolent. Cell death levels were consistent across the histologies. B, Representative images of Ki67 (left panels) and cPARP (right panels) immunohistochemical staining of high (LT103; top panels), medium (LT98; middle panels) and low (LT104; bottom panels) proliferative tumours. Immunohistochemical stains were counterstained with haematoxylin. LT103 (high proliferative tumour) and LT98 (medium proliferative tumour) represent SCC samples whereas LT104 (low proliferative tumour) is an ADC. Scale bars = 100 μm.

Figure 2. Establishment of optimal explant culture conditions**.** A, Evaluation of proliferation and cell death levels with increasing time of explant culture. The % Ki67 (left graphs) and % cPARP (right graphs) immunohistochemical staining of five NSCLC *ex-vivo* explants over time are shown. The staining values were generated from the uncultured tumour in its native state and from explants from the same tumour at 24, 48 and 72 hours of culture after an initial recovery of 16-20 hours. The graphs at the top show individual values for each of the five tumours. The graphs on the bottom indicate pooled mean values for the five samples ± 95% CI. Page's L nonparametric trend test showed a negative trend for Ki67 staining with increasing culture time (P = 0.01; L statistic = 143) and a positive trend for cPARP staining with increasing culture time (P = 0.05; L statistic = 140). B, Evaluation of % Ki67 and % cPARP staining with varying FCS concentrations. The % Ki67 (left graphs) and % cPARP (right graphs) immunohistochemical staining of five NSCLC *ex-vivo* explants over time are shown. The staining values were generated from the uncultured tumour in its native state and from explants from the same tumour cultured in varying FCS concentrations for 24 hours after an initial recovery of 16-20 hours. The graphs at the top show individual values for each of the five tumours. The graphs on the bottom indicate pooled mean values for the five samples ± 95% CI. Page's L nonparametric trend test showed no significant difference for Ki67 or cPARP staining with varying FCS concentration. C, Summary of the effect of

cultivation. The % Ki67 (left graph) and % cPARP (right graph) staining were determined for twenty-one explant cultures. The box and whiskers plots show the data for uncultured tumours compared to tumours cultured for 24 hrs + 16-20 hrs of recovery in 1% FCS. The boxes extend from the 25th to 75th percentiles and the lines in the middle of the boxes represent the median. The whiskers extend from the smallest to the largest values.

Figure 3. NSCLC explant response to cisplatin. A, Fold Cell Death relative to control of 17 NSCLC explant cultures treated with a dose range (0-50 μM) of cisplatin. The % cPARP staining of each sample was quantitated within explants from the same tumour cultured in carrier control (DMF) or increasing cisplatin concentrations (1 μM, 10 μM and 50 μM) for 24 hours after an initial recovery of 16-20 hours. The value for each treatment was divided by the carrier control to obtain a fold change. B, Kaplan-Meier patient survival correlated with sensitivity of explants to cisplatin at 50 μM. Data was evaluated for 25 patients/explants (Table S1). The threshold of sensitivity/resistance to the drug was determined using a ROC curve (Figure S4A). The Mantel Cox log-rank test identified a statistically significant relationship ($P < 0.019$) between patient survival and cisplatin sensitivity. C, Correlation of response to cisplatin in explant culture with tumour stage (left panel) and histology (right panel). The box and whiskers plots show data for different in % cPARP staining in response to 50 μM cisplatin compared to control treatment for each explant relative to tumour stage/histology. The box extends from the 25th to 75th percentiles and the lines in the middle of the boxes represent the median. The whiskers extend from the smallest to the largest values. The Jonckheere-Terpstra test for ordered alternatives showed a significant negative trend ($P = 0.008$) between increasing stage and cisplatin response. Correlation of tumour histology with cisplatin response demonstrated statistically significant differences between SCC samples and both ADC and AC types.

Figure 4. Pt ion distribution in cisplatin sensitive and resistant explants. A, Cisplatin resistant explant (LT31) and (B) cisplatin sensitive explant (LT88). Both samples were treated with 10 μM cisplatin. Serial sections of explants stained with H&E staining are shown in the top left panels, and immunohistochemical staining with antibodies for MNF116 (top middle panels), cPARP (top right panels) and Ki67 (bottom left panels) are also shown. LA-ICP-MS samplings to indicate the distribution of Pt ions within each explant are shown in the bottom right panels. The white lines indicate tumour areas as determined by H&E and MNF116 staining. Scale bars = 100 μm.

Figure 5. TP53 expression. A, Immunohistochemical staining of explants treated with cisplatin demonstrating tumours with constitutively high levels of nuclear TP53 in tumour cells (LT18, LT27 and LT23) or low levels of TP53 (LT116). Scale bars = 100 μm. B, Immunohistochemical staining and quantitation of nuclear p53 staining in a $TP53^{WT}$ explant sample demonstrating dose-dependent TP53 expression following cisplatin treatment. The graph shows the % mean labelling index of TP53 ± SD following treatment of the tumour sample with increasing doses of cisplatin ($P < 0.0001$). Scale bars = 100 μm. C, Correlation of intrinsic proliferation index with TP53 immunohistochemical staining. The graph shows the % Ki67 staining of tumours classified according to TP53 immunohistochemical staining. Each circle represents one sample. D, Induction of cell death, as assessed by cPARP staining (left graph), and reduction of proliferation (right graph), as assessed by Ki67 staining, upon 50 μM cisplatin treatment of 26 NSCLC *ex-vivo* explants stratified according to their ability to induce TP53 expression upon treatment with the drug. The data show that TP53-inducible tumours have a significantly reduced ability to undergo cell death in response to cisplatin compared to TP53 non-inducible tumours. The majority of these tumours are of the SCC subtype.

Figure 6. Response to TRAIL. A, Fold cell death induction in response to 1 μg/ml of TRAIL, 50μM Cisplatin or a combination of the two relative to the carrier control is shown. The % cell death of twelve *ex-vivo* explant cultures as determined by cPARP staining was determined after each treatment for 24 hours after an initial recovery of 16-20 hours. These values were divided by the value for each carrier control to calculate the fold difference. B, Representative images of cPARP staining of LT83, LT18 and LT22 treated with 1 μg/ml of TRAIL, 50μM Cisplatin or a combination of the two. Scale bars = 100 μm.

Table 1. Summary of patients' characteristics and tumours used for this study.

Characteristic	Number of patients/tumours	% of patients/tumours
Sex		
Male	23	56.1
Female	18	43.9
Age		
Median	70	
Range	54-85	
Histology		
Adenocarcinoma	18	43.9
Squamous Cell Carcinoma	20	48.8
Large Cell Carcinoma	0	0
Atypical Carcinoid	3	7.3
Stage		
IA	6	14.7
IB	8	19.5
IIA	8	19.5
IIB	9	21.9
IIIA	8	19.6
IIIB	1	2.4
IV	1	2.4

Tumour samples were collected from consented patients undergoing lung surgery at Glenfield Hospital, Leicester. Clinical data, histology and stage were provided by official histopathology reports submitted by consultant pathologists at University Hospitals of Leicester, UK.

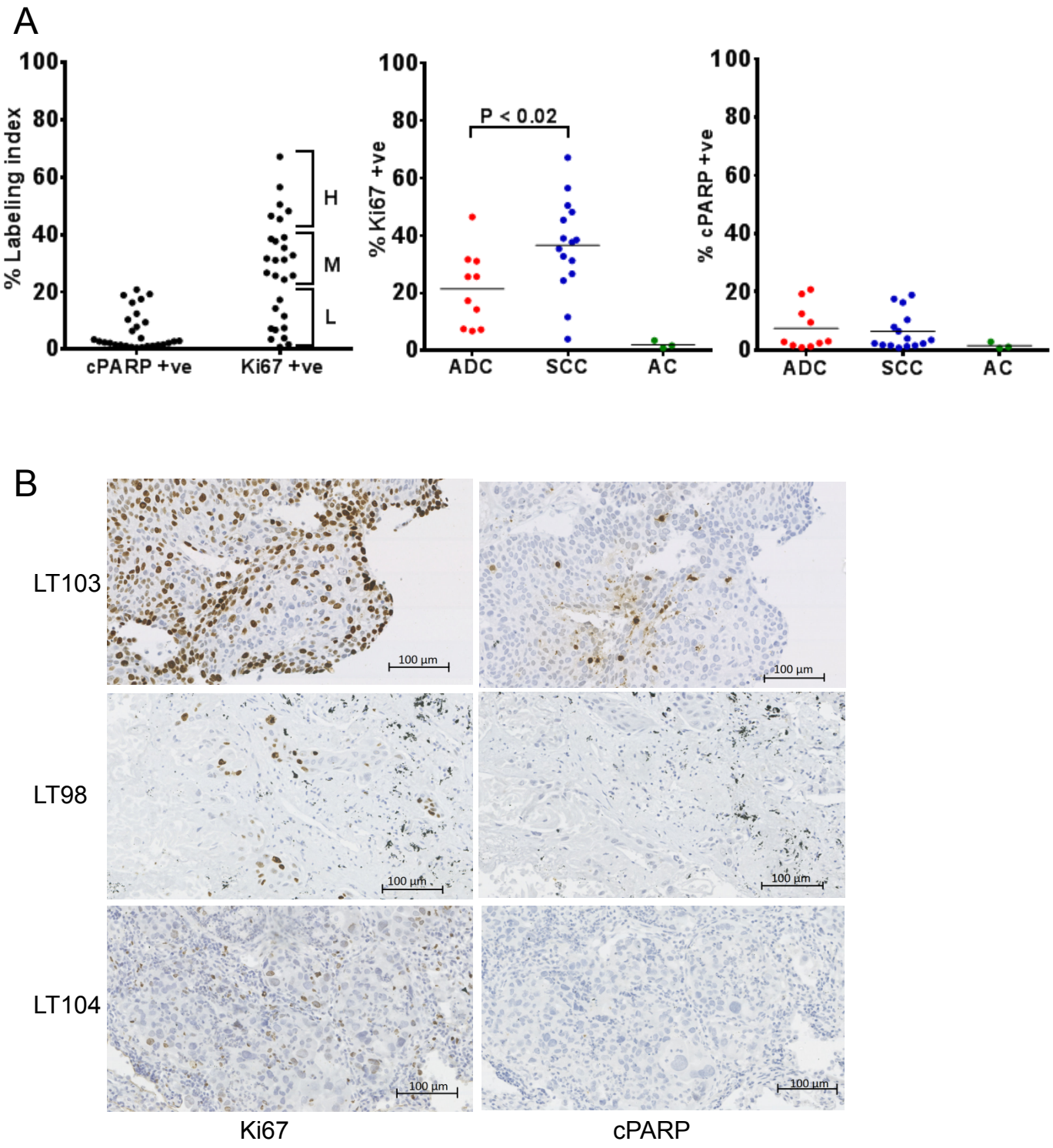
A
% Labeling index
100
80
60
40
20
0
H
M
L
cPARP +ve
Ki67 +ve
% Ki67 +ve
P < 0.02
ADC
SCC
AC
% cPARP +ve
B
LT103
LT98
LT104
100 µm
Ki67
cPARP

Figure 1

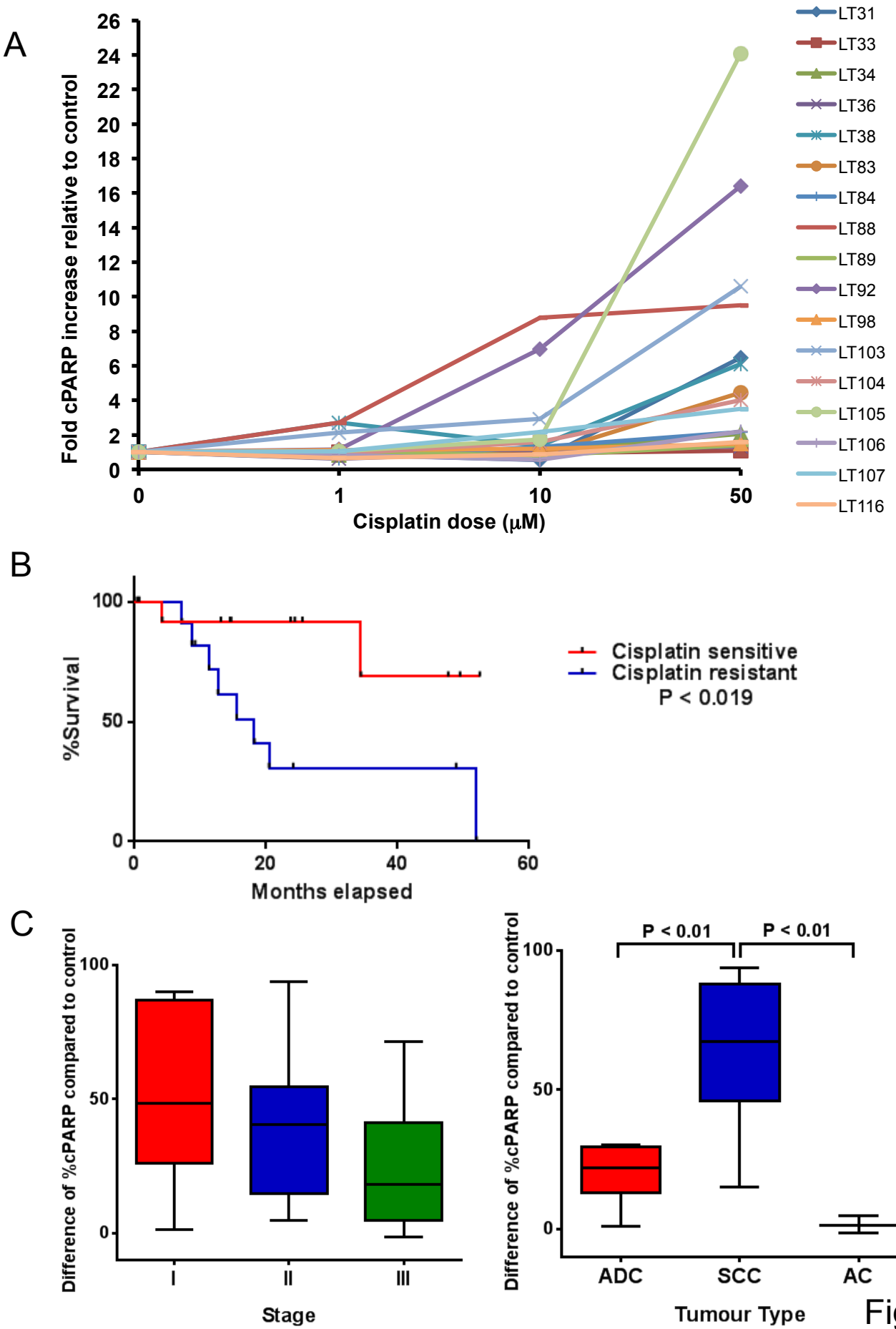
A
Fold cPARP increase relative to control
Cisplatin dose (μM)
LT31
LT33
LT34
LT36
LT38
LT83
LT84
LT88
LT89
LT92
LT98
LT103
LT104
LT105
LT106
LT107
LT116
B
%Survival
Months elapsed
Cisplatin sensitive
Cisplatin resistant
P < 0.019
C
Difference of %cPARP compared to control
Stage
I
II
III
P < 0.01
P < 0.01
Tumour Type
ADC
SCC
AC

Figure 3

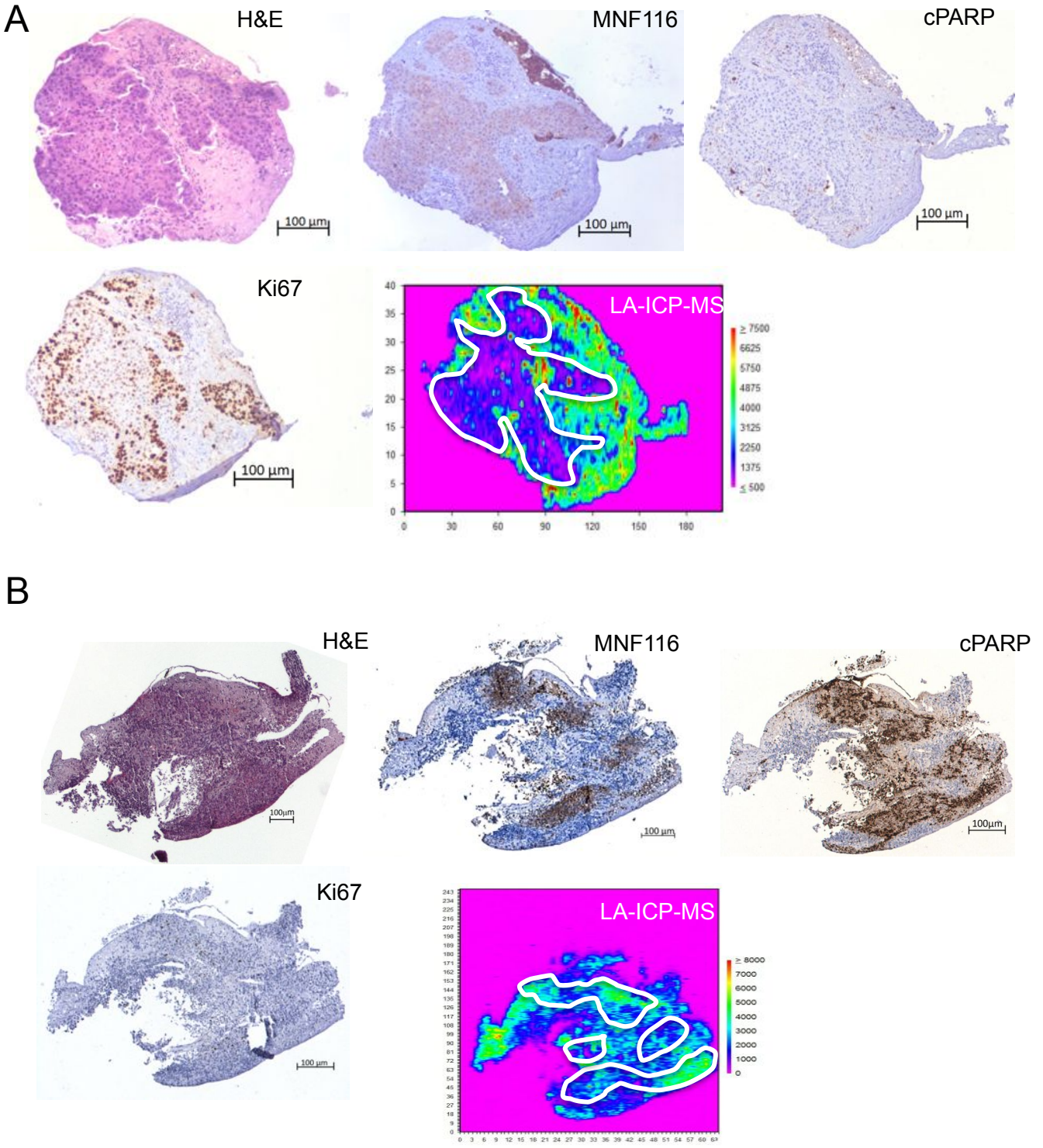
A
H&E
MNF116
cPARP
100 µm
Ki67
LA-ICP-MS
≥ 7500
6625
5750
4875
4000
3125
2250
1375
≤ 500
B
H&E
MNF116
cPARP
100µm
Ki67
LA-ICP-MS
≥ 8000
7000
6000
5000
4000
3000
2000
1000
0

Figure 4

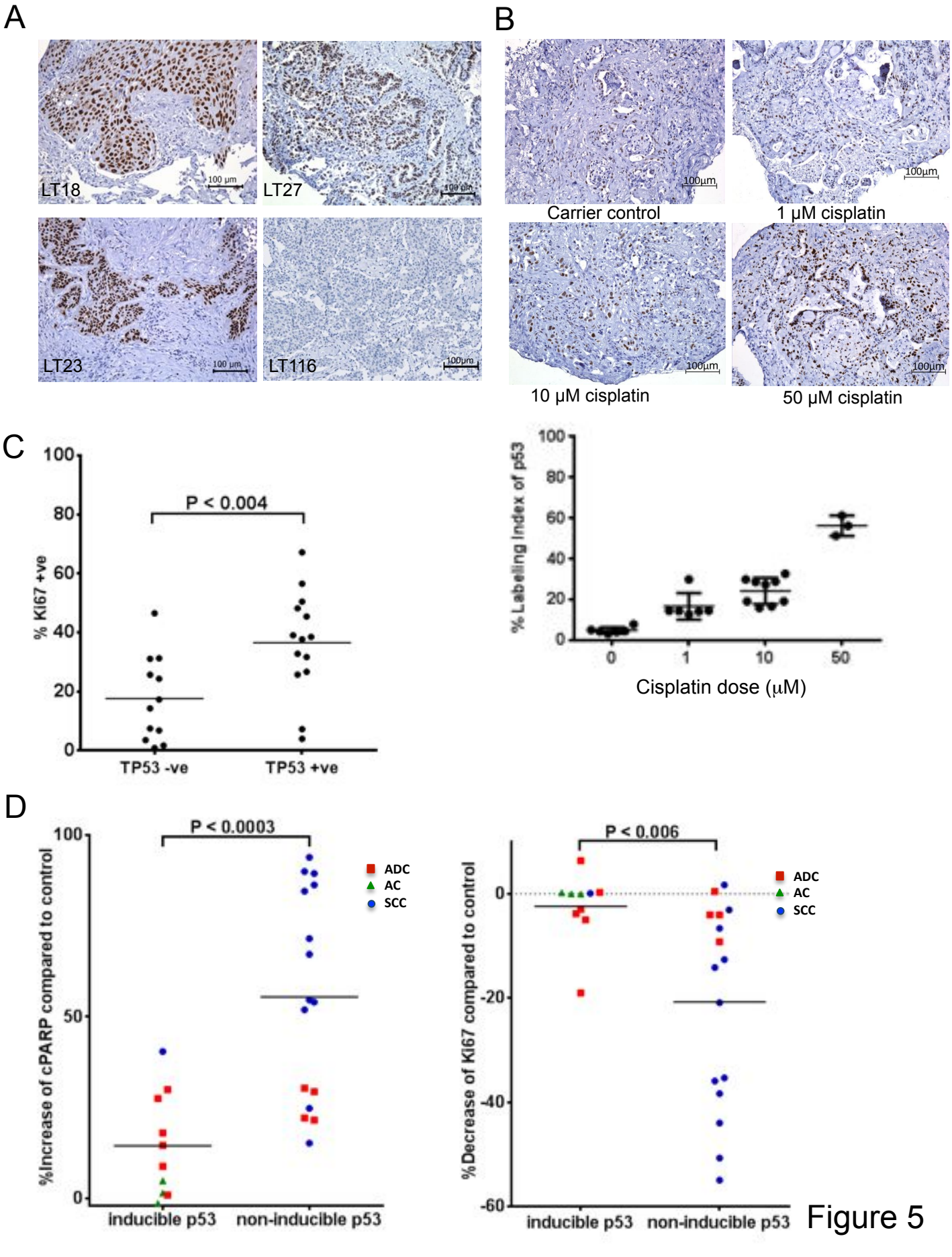
A
LT18
LT27
LT23
LT116
B
Carrier control
1 μM cisplatin
10 μM cisplatin
50 μM cisplatin
C
P < 0.004
% KI67 +ve
TP53 -ve
TP53 +ve
% Labeling Index of p53
Cisplatin dose (μM)
D
P < 0.0003
%Increase of cPARP compared to control
ADC
AC
SCC
inducible p53
non-inducible p53
P < 0.006
%Decrease of KI67 compared to control

Figure 5

A

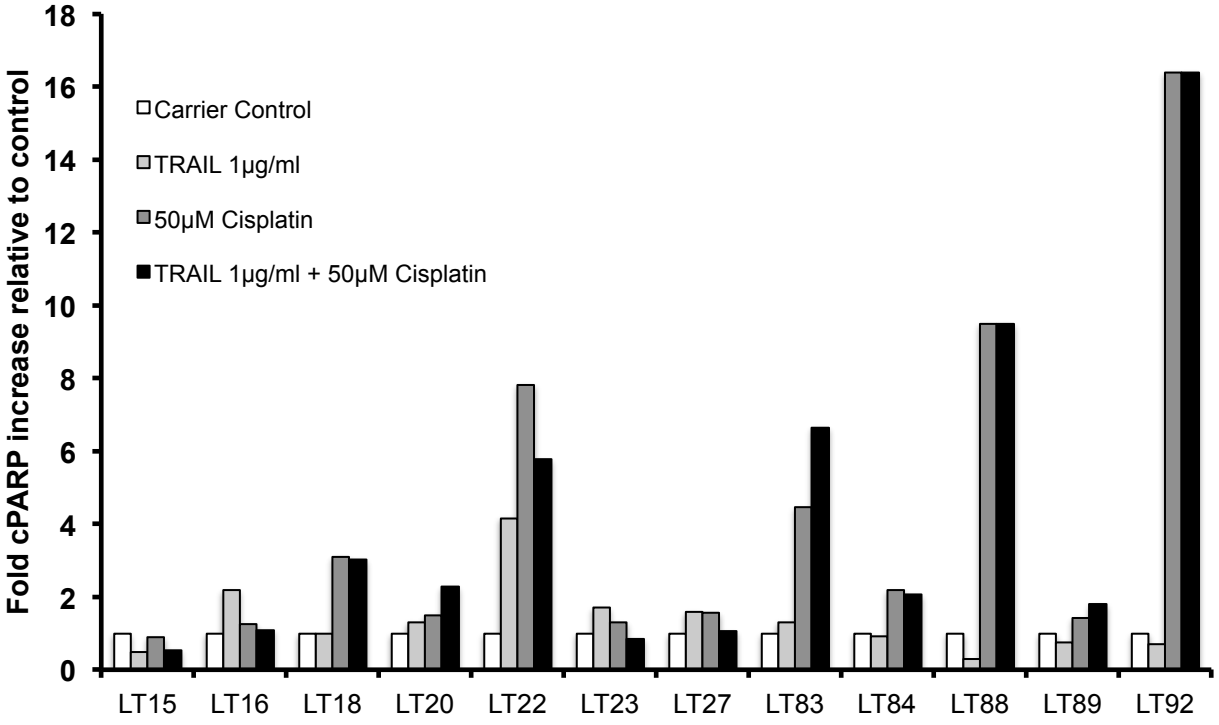
Fold cPARP increase relative to control
18
16
14
12
10
8
6
4
2
0
Carrier Control
TRAIL 1µg/ml
50µM Cisplatin
TRAIL 1µg/ml + 50µM Cisplatin
LT15
LT16
LT18
LT20
LT22
LT23
LT27
LT83
LT84
LT88
LT89
LT92

B

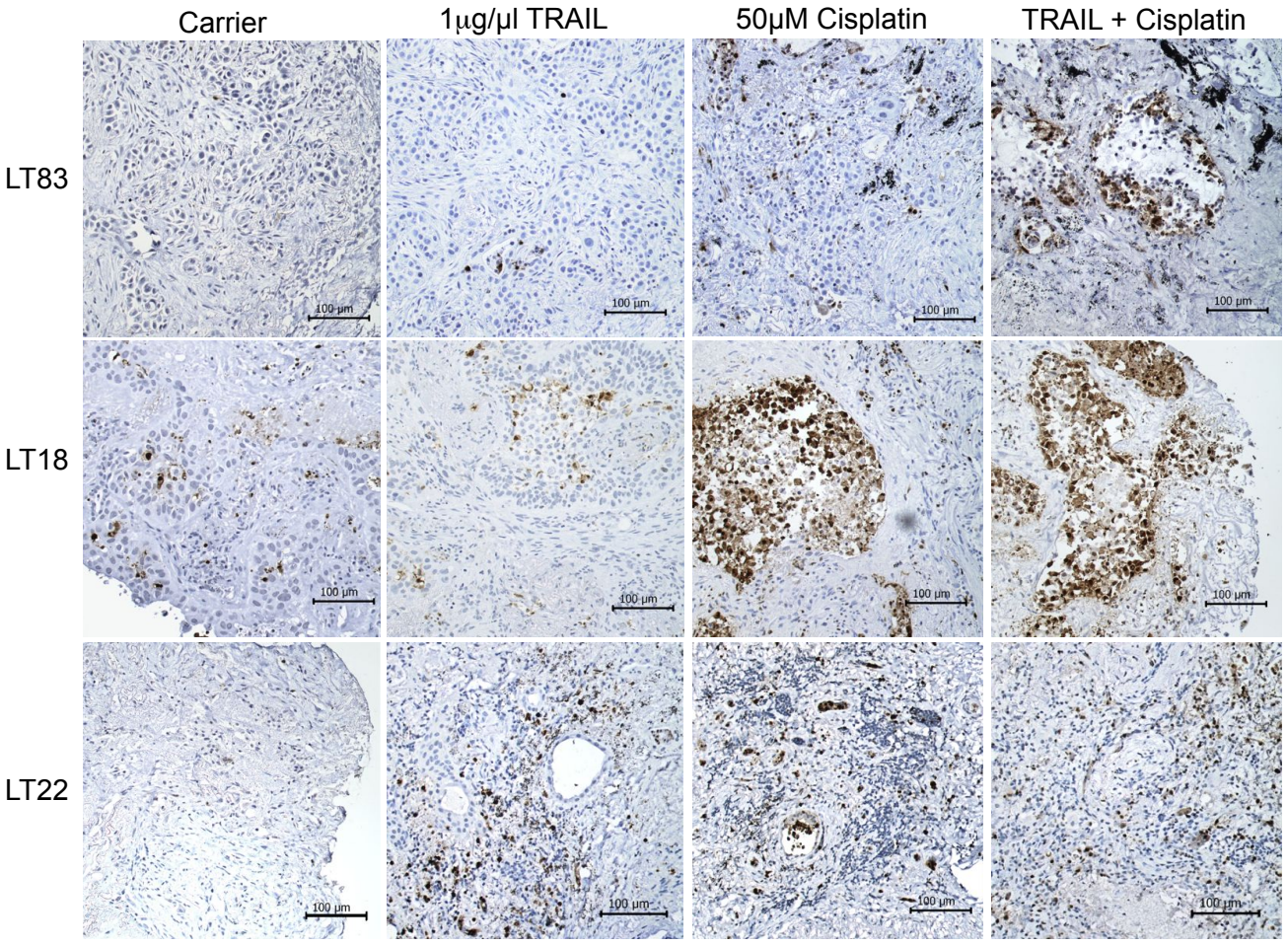
Carrier
1µg/µl TRAIL
50µM Cisplatin
TRAIL + Cisplatin
LT83
LT18
LT22
100 µm

Figure 6